A Digitally Implemented Phase-Locked Loop Detection Scheme for Analysis of the Phase and Power Stability of a Calibration Tone

A. C. Densmore
Telecommunications Systems Section

A digital phase-locked loop (PLL) scheme is described which detects the phase and power of a high SNR calibration tone. The digital PLL is implemented in software directly from the description given in this article. It has been used to evaluate the stability of the Goldstone Deep Space Station open loop receivers for Radio Science. Included is a derivation of the Allan variance sensitivity of the PLL imposed by additive white Gaussian noise; a lower limit is placed on the carrier frequency.

I. Introduction

To facilitate the evaluation of the phase and gain stability of the DSN open loop receivers for Radio Science, a detection scheme was developed. Radio Science objectives accommodated include the study of the atmospheres and ionospheres of the planets and satellites by means of radio occultation of a signal sent from a spacecraft and received at Earth (at a Deep Space Station). The stability of the receivers directly affects the quality of the science return of the experiment.

The process of testing station stability supported by this detection scheme involves three stages. The first stage consists of running the test and digitally recording the calibration tone on tape. The tone is generated at 2.3 GHz or 8.4 GHz and is downconverted to an intermediate frequency inside the antenna, cabled to the Signal Processing Center, where it is further downconverted by the IF-to-video converter, and then sampled by an analog-to-digital converter and recorded on tape. The second stage in testing station stability is detection of the calibration tone frequency (phase) and power as functions of time from the voltage samples recorded on the tape; the detection is accomplished by computer software that directly implements the scheme presented in this article. The detected frequency and power are stored in a computer data file. The last stage involves postprocessing the detected data file to yield suitable statistical measures of the calibration tone stability. These measures include Allan variance [4] as a measure of frequency stability, phase variation plotted as a function of time, power spectral plots of the detected frequency and tone power, and simple plots of the detected frequency and tone power. The scheme presented in this article is an implementation of the second stage: detection of the frequency (phase) and power of the tone. This article does not discuss the details of the latter postprocessing stage, although the theoretical noise-limited Allan variance is derived.

The input signal intended for this detection scheme is assumed specifically to consist of a single tone centered in a narrow (relative to the sample rate) band of noise with a high signal-to-noise ratio. Recent DSN calibration tone tests have

provided a 40 to 50 dB-Hz SNR with a 100-Hz noise bandwidth which corresponds to a 20- to 30-dB signal-to-noise ratio. These values are high enough to allow practical use of a noncoherent square-law power detector.

In Sections III and IV, the linearized, continuous-time model of the detector is analyzed. The continuous-time analysis of the discrete-time phase-locked loop (PLL) is justified by the assumption that the product of the PLL loop noise bandwidth and the sample period is much less than unity, i.e., $PLLBW \cdot T \ll 1$. Section II discusses the block diagram and its digital implementation, from which the software is directly written; the software is the implementation of the PLL presented in this article and detects the phase and power information from the previously recorded calibration tone voltage samples. The concluding Section V cites some of the results obtained using this scheme for DSN tests.

II. Implementation

The heart of this detection scheme is a second order phase-locked loop. In this section, the block diagram is presented and described.

Figure 1 is the block diagram of the PLL detector. The left-hand side of Fig. 1 is a noncoherent tone-power detector used to normalize the amplitude of the input sinusoid; it is described in further detail in Section IV. The upper right-hand corner of Fig. 1 is the phase-locked loop circuit; it consists of a loop filter, a numerically controlled oscillator (NCO), a mixer, and a low-pass filter (LPF_1). The frequency of the NCO is directly proportional to its numerical input. The mixer is used as a coherent phase detector, and the low-pass filter serves as a harmonic rejection filter by assisting the loop filter in attenuating the mixer second harmonic to afford greater choice of input carrier frequency, as explained in Section IIIC. The PLL is described in further detail in Section III. In order to detect that the loop is in lock, a lock detector is implemented, as shown in the lower right-hand corner of Fig. 1. Assuming that the input sinusoid amplitude is properly normalized, the lock detector output takes the value unity in the phase-locked state. If the loop is offset by a phase error ϕ, the lock detector output takes the value $\cos\phi$.

The overall detector is implemented in software directly from the block diagram. A bilinear s- to z-domain transformation is used to implement each function in discrete time given the corresponding s-domain transfer function:

$$s = \left(\frac{2}{T}\right)\left(\frac{1 - z^{-1}}{1 + z^{-1}}\right) \tag{1}$$

where T is the sample period in seconds.

This transform has the property that a single pole low-pass filter transformed to a discrete time recursive filter appears nearly as the same single pole filter at frequencies less than one-tenth the sampling rate and has a zero at half the sampling rate.

Below are the bilinear transforms of the loop filter, the high-pass filter, and the low-pass filters. Canonic form digital implementations for each are given in Fig. 2.

Loop filter:

$$s\text{-domain: } F(s) = \frac{1 + as}{bs} \tag{2}$$

$$\text{bilinear transform: } F(z) = \frac{T + 2a}{2b}\,\frac{1 + z^{-1}\dfrac{T - 2a}{T + 2a}}{1 - z^{-1}} \tag{3}$$

High-pass filter:

$$s\text{-domain: } H(s) = \frac{1}{1 + \dfrac{c}{s}} \tag{4}$$

$$\text{bilinear transform: } H(z) = \frac{2}{2 + cT}\,\frac{1 - z^{-1}}{1 - z^{-1}\dfrac{2 - cT}{2 + cT}} \tag{5}$$

Low-pass filter:

$$s\text{-domain: } K(s) = \frac{1}{1 + \dfrac{s}{d}} \tag{6}$$

$$\text{bilinear transform: } K(z) = \frac{dT}{2 + dT}\,\frac{1 + z^{-1}}{1 - z^{-1}\dfrac{2 - dT}{2 + dT}} \tag{7}$$

III. Frequency Detection

Presented in this section is a detailed discussion of the choice of loop parameters and a discussion of the use of Allan variance as a measure of frequency stability. A lower limit on the allowable input carrier frequency is derived by consideration of its effect on the Allan variance measure.

A. Linear Loop Analysis

Consider the second order, baseband, linear PLL in the s-domain. The PLL input is the radian phase $\theta(t)$, and the output is the detected radian frequency $\hat{\omega}(t)$. The forward gain path is the loop filter, $F(s) = (1 + as)/bs$, and the negative feedback path is an integrator, $G(s) = 1/s$. By Mason's rule, the closed loop transfer function [3] is given by

$$L(s) = \frac{F(s)G(s)}{1 + F(s)G(s)} = \frac{1 + as}{1 + as + bs^2} \tag{8}$$

The one-sided loop noise bandwidth is given by the following expression [1]:

$$PLLBW = \frac{1}{2\pi}\int_0^\infty |L(j\omega)|^2\, d\omega = \frac{a^2 + b}{4ab} \tag{9}$$

In order to evaluate the output of the PLL, the transfer function from input phase to output detected frequency is derived by Mason's rule:

$$W(s) \doteq \frac{\hat{\omega}_{out}}{\theta_{in}}(s) = \frac{s(1 + as)}{1 + as + bs^2} \tag{10}$$

It is convenient to define the parameter $R \doteq a^2/b$. By manipulating Eq. (9), the following relations are revealed:

$$a = \frac{R + 1}{4(PLLBW)}, \qquad b = \frac{a^2}{R} \tag{11}$$

The system characteristic equation is:

$$1 + \frac{1}{Q}\left(\frac{s}{\omega_n}\right) + \left(\frac{s}{\omega_n}\right)^2 \tag{12}$$

where

$$Q = \frac{1}{\sqrt{R}} \tag{13}$$

This reveals that R is the loop damping parameter. Jaffee and Rechtin [2] specify optimum loop performance with $R = 2$ when the initial phase is unknown but uniformly distributed as a random variable. Unless stated otherwise, R is assumed to equal 2 throughout the remainder of this article. $R = 2$ makes the system slightly underdamped.

B. Allan Variance

Allan variance is a statistical measure of the frequency stability of a signal. It is a measure of fractional frequency fluctuations rather than absolute frequency fluctuations; a fluctuation of 1 Hz in a 10-GHz tone represents a lower Allan variance than the same 1-Hz fluctuation in a 10-MHz tone. The sensitivity of the Allan variance measure is limited by the input noise; with too much noise the Allan variance measures only the noise. The following defines the theoretical Allan variance in the case of detecting with the second order PLL the frequency of a pure tone with a high signal-to-noise ratio in a band of additive white Gaussian noise (AWGN).

A convenient estimate of Allan variance is given below as defined in Eq. (4.22) of [4]:

$$\sigma_y^2(\tau) = \frac{1}{2(M-1)}\sum_{i=1}^{M-1}[\bar{y}_{i+1}(\tau) - \bar{y}_i(\tau)]^2 \tag{14}$$

where

$$\bar{y}_i(\tau) = \frac{1}{\tau}\int_{(i-1)\tau}^{i\tau}\frac{\hat{\omega}(t)}{2\pi\nu_0}\,dt$$

where ν_0 is the nominal frequency of the calibration tone prior to any downconversion; $\sigma_y(\tau)$ is the RMS value of all the two-sample variances taken over the entire set of data. A single two-sample variance is given by $[\bar{y}_{i+1}(\tau) - \bar{y}_i(\tau)]/\sqrt{2}$. The two-sample variance function, $p(t,\tau)$, is defined as the difference between two consecutive averages of a function, each taken over a period τ and normalized by $\sqrt{2}$.

$$p(t,\tau) = \begin{cases} \dfrac{-1}{\tau\sqrt{2}}, & -\tau \leqslant t < 0 \\ \dfrac{1}{\tau\sqrt{2}}, & 0 \leqslant t < \tau \\ 0 & \text{otherwise} \end{cases} \tag{15}$$

The theoretical Allan variance of the fractional detected frequency at the output of the PLL is the statistical mean of the square of the convolution of the two-sample variance function $p(t,\tau)$, with the fractional detected frequency output of the PLL $\hat{f}(t)/\nu_0 = \hat{\omega}(t)/2\pi\nu_0$.

$$\sigma_y^2(\tau) = E\left\{[(\hat{f}(t)/\nu_0) * p(t,\tau)]^2\right\} \tag{16}$$

$$\doteq \text{power in } (\hat{f}(t)/\nu_0) * p(t,\tau)$$

$$= \int_{-\infty}^{\infty} S(f)P(f,\tau)df \qquad (17)$$

where $P(f,\tau)$ = the power spectrum of the two-sample variance function [squared magnitude of the Fourier transform of $p(t,\tau)$]:

$$P(f,\tau) = \frac{2\sin^4 \pi\tau f}{(\pi\tau f)^2} \qquad (18)$$

and $S(f)$ = the power spectrum of the detected fractional frequency due to AWGN about a pure tone input to the PLL:

$$S(f) = S_\theta(f)\left|\frac{W(j2\pi f)}{2\pi\nu_0}\right|^2 \qquad (19)$$

where $S_\theta(f)$ = the phase power spectrum input to the PLL due to AWGN about a pure tone with high SNR.

Narrowband, high SNR AWGN about a pure carrier represents a white phase noise power spectrum, $S_\theta(f)$, about the carrier with the same narrow band.

$$S_\theta(f) = \frac{1}{2SNR}\ (\text{rad}^2/\text{Hz})\,; \qquad |f| < B_N/2 \qquad (20)$$

where B_N = input noise bandwidth. By substitution,

$$\sigma_y^2(\tau) = \int_{-\infty}^{\infty} \frac{1}{8\pi^2\nu_0^2\, SNR}\left|\frac{j2\pi f(1+aj2\pi f)}{1+aj2\pi f - b4\pi^2 f^2}\right|^2 \times \frac{2\sin^4\pi\tau f}{(\pi\tau f)^2}\, df \qquad (21)$$

Numerical integration yields

$$\sigma_y^2(\tau) \Rightarrow \frac{3(PLLBW)}{4\pi^2\nu_0^2\, SNR\, \tau^2}\,; \qquad \tau(PLLBW) \gg 1 \qquad (22)$$

On a log-log plot of $\sigma_y(\tau)$ as a function of τ, the noise-limited Allan variance plotted for several detection loop bandwidths takes the shape of parallel lines each with a negative unity slope; this is shown in Fig. 3 with $\nu_0^2\, SNR \approx 7.6 \times 10^{20}$. The individual plots are only shown for τ such that $\tau(PLLBW) > 1$; this is the only domain over which the SNR-limited Allan variance log-log plot has the negative unity slope. By plotting only over this domain, any peculiar shape immediately draws attention to some phenomenon other than high SNR AWGN. Note that the reduction of detection loop bandwidth to improve the Allan variance sensitivity further limits the minimum τ over which the Allan variance may be evaluated.

C. Minimum Input Carrier Frequency

Consideration of the significance of the mixer sum product places a lower limit on the input carrier frequency for this detection scheme without acting as a detriment to the Allan variance frequency stability measurement. This serves as a criterion for selecting the carrier frequency. It is assumed that sampling does not disturb the two-to-one second- to first-carrier harmonic frequency relationship. The criterion is that the Allan variance due to the harmonic term alone must be much less than the Allan variance due to the phase difference term alone.

First let us consider the phase difference term. The Allan variance was derived previously and is summarized below, but here absolute rather than fractional frequency variance is considered, so the ν_0^2 term is removed from Eq. (22).

$$\sigma_y^2(\tau)\Big|_{\theta(t),\text{abs}} = \frac{3(PLLBW)}{4\pi^2 SNR\tau^2} \qquad (23)$$

Now consider the (absolute) Allan variance due to the second harmonic tone:

$$\sigma_y^2(\tau)\Big|_{2f_0,\,\text{abs}} = \int_{-\infty}^{\infty} S_2(f)P(f)\,df \qquad (24)$$

Recall that

$$P(f) = \frac{2\sin^4 \pi\tau f}{(\pi\tau f)^2} \qquad (25)$$

$S_2(f)$ is the power spectrum at the detector output due only to the second harmonic term. Assuming zero loop gain at the second harmonic frequency, $S_2(f)$ is the product of the power spectrum of the second harmonic tone, the harmonic rejection filter response, and the loop filter response.

$$S_2(f) = P\left[\frac{1}{2}\delta(f+2f_0) + \frac{1}{2}\delta(f-2f_0)\right]\left|LPF_1(j2\pi f)\right|^2\left|\frac{F(j2\pi f)}{2\pi}\right|^2 \qquad (26)$$

$P = 1/2$ is the power in the second harmonic tone at the output of the mixer. Assuming the second harmonic is much higher than the corner frequencies of the filters, the follow-

ing approximations hold. The corner frequency of the harmonic rejection filter is made equal to ten times the one-sided loop noise bandwidth so as to only negligibly affect the loop response.

$$\left|LPF_1(j2\pi 2f_0)\right|^2 = \frac{1}{1+(2f_0/10\,PLLBW)^2} \Rightarrow \frac{25\,PLLBW^2}{f_0^2} \tag{27}$$

$$\left|\frac{F(j2\pi 2f_0)}{2\pi}\right|^2 \Rightarrow \left(\frac{2R\,PLLBW}{\pi(R+1)}\right)^2 \tag{28}$$

$$P(f) \Rightarrow \leqslant \frac{2}{(\pi\tau 2f_0)^2} \tag{29}$$

By substituting Eqs. (26)–(29) into Eq. (24) and comparing Eqs. (23) and (24),

$$\sigma_y^2(\tau)\Big|_{2f_0} \ll \sigma_y^2(\tau)\Big|_{\theta(t)} \tag{30}$$

$$\frac{25\,PLLBW^4\,R^2}{\pi^4 f_0^4 (R+1)^2\tau^2} \ll \frac{3\,PLLBW}{4\pi^2 SNR\tau^2}$$

Solving for carrier frequency yields the following lower limit imposed by Allan variance detriment by the second carrier harmonic.

$$f_0\Big|_{R=2} \gg SNR^{1/4} \times PLLBW^{3/4} \tag{31}$$

IV. Power Detection

The amplitude detector in Fig. 1 consists of a square-law power detector preceded by a DC-blocking high-pass filter, and sinusoidal amplitude is estimated as the square root of twice the detected power: $A \approx \sqrt{2(A^2/2 + \sigma_N^2)}$. The perfectly smoothed square-law detected power is $A^2/2 + \sigma_N^2$, but there is an uncertainty in the power detector output due to the finite smoothing of the post-detection filter; the purpose of this section is to specify the uncertainty.

The signal input to the detector is assumed to have the form $A\cos\omega_C t + n(t)$, where $n(t) = \sqrt{2}n_c(t)\cos\omega_C t + \sqrt{2}n_s(t)\sin\omega_C t$. By narrowband noise theory, n_c and n_s are zero mean, uncorrelated, independent, low-pass, band-limited AWGN signals each with a two-sided bandwidth B_N and a two-sided power spectral density $N_0/2$. B_N is assumed to be much smaller than the sample rate.

In [5] it is shown that the two-sided power spectrum at the output of the mixer is given by the following. Equation (12-62) of [5] is rewritten below in the terms used in this article.

$$S_{yy}(f) = (P + N_0B_N)^2\,\delta(f) + \begin{cases} 2PN_0, & 0 < |f| \leqslant B_N/2 \\ 0 & \text{otherwise} \end{cases} + \begin{cases} N_0^2(B_N - |f|), & 0 < |f| \leqslant B_N \\ 0 & \text{otherwise} \end{cases} \tag{32}$$

Second harmonic terms are neglected here with the assumption that the postdetection filter removes them, and $P = A^2/2$.

Generally the postdetection low-pass filter noise bandwidth, $AGCBW$, is much smaller than the input noise bandwidth, i.e., $AGCBW \ll B_N$. This allows the approximation, except for the impulse at the origin, that the power spectrum at the mixer output, $S_{yy}(f)$, is a constant equal to its value near DC. In this case the total noise power at the output of the postdetection filter is given by the following expression:

$$P_N \approx 2(2PN_0 + N_0^2B_N)AGCBW \tag{33}$$

The power in the desired signal is the DC component.

$$P_S = (P + N_0B_N)^2 \tag{34}$$

The signal to total noise power ratio at the output of the square-law power detector is given by

$$SNR_{PD} \doteq \frac{P_S}{P_N} = \frac{(SNR + B_N)^2}{2(2SNR + B_N)AGCBW} \tag{35}$$

where $SNR = P/N_0$ is the input signal to noise density power ratio. Consider the normalized postdetection noise variance:

$$\sigma^2 \doteq \frac{1}{SNR_{PD}} \tag{36}$$

A simple definition of detection uncertainty (error bar) is given by

$$2\sigma\Big|_{\mathrm{dB}} = 40 \log (1 + \sigma) \tag{37}$$

Substituting for σ yields the error bar for the power detection or tone power detection uncertainty:

$$2\sigma\Big|_{\mathrm{dB}} = 40 \log \left(1 + \sqrt{\frac{2(2SNR + B_N)AGCBW}{(SNR + B_N)^2}}\right) \tag{38}$$

V. Conclusion

The digital PLL detection scheme presented in this article has been used to evaluate the stability of the DSN open loop receivers as described in the introduction. The results obtained have been very satisfactory. The discoveries made using this scheme for calibration tone stability tests include the detection of a 200-millihertz frequency-modulated tone in an 8.4-GHz carrier and calibration tone frequency offsets on the order of microhertz. This scheme has been used to evaluate tone generator–receiver system phase stability with a root Allan variance sensitivity of 10^{-17} at a 1000-second integration time. The accuracy of this detection scheme depends only on the accuracy with which the software records individual parameters. FORTRAN double precision variables are accurate up to 14 significant digits.

The processing time required to detect from a three-hour digital recording the phase and power of each of two tones recorded simultaneously on separate channels at a 200-Hz sample rate, and to complete the differential and Allan variance postprocessing, was approximately eight hours using a FORTRAN 77 compiler on the PRIME 550 CPU in the JPL Radio Occultation Data Analysis (RODAN) facility.

References

[1] G. C. Newton, L. A. Gould, and J. F. Kaiser, *Analytical Design of Linear Feedback Controls*, New York: Wiley, 1957.

[2] R. M. Jaffee and E. Rechtin, "Design and Performance of Phase Locked Circuits Capable of Near-Optimum Performance Over a Wide Range of Input Signal and Noise Levels," *IRE Transactions on Information Theory*, vol. IT-1, pp. 66–76, March 1955.

[3] R. C. Tausworthe, *Theory and Practical Design of Phase Locked Receivers*, vol. I, JPL Technical Report 32-819, Jet Propulsion Laboratory, Pasadena, California, February 1966.

[4] J. Rutman, "Characterization of Phase and Frequency Instabilities in Precision Frequency Sources: Fifteen Years of Progress," *Proc. IEEE*, vol. 66, no. 9, pp. 1048–1075, September 1978.

[5] W. B. Davenport, Jr., *An Introduction to the Theory of Random Signals and Noise*, New York: McGraw-Hill, pp. 259–263, 1958.

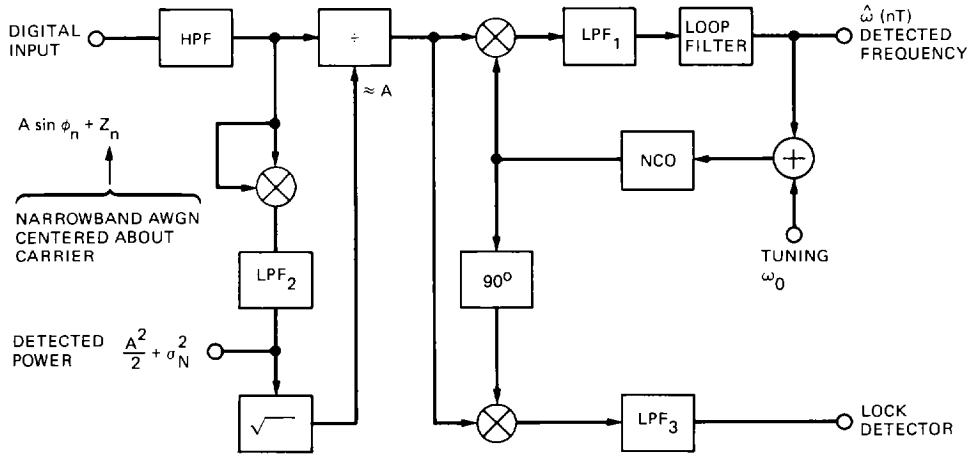

Fig. 1. Functional block diagram of PLL detector

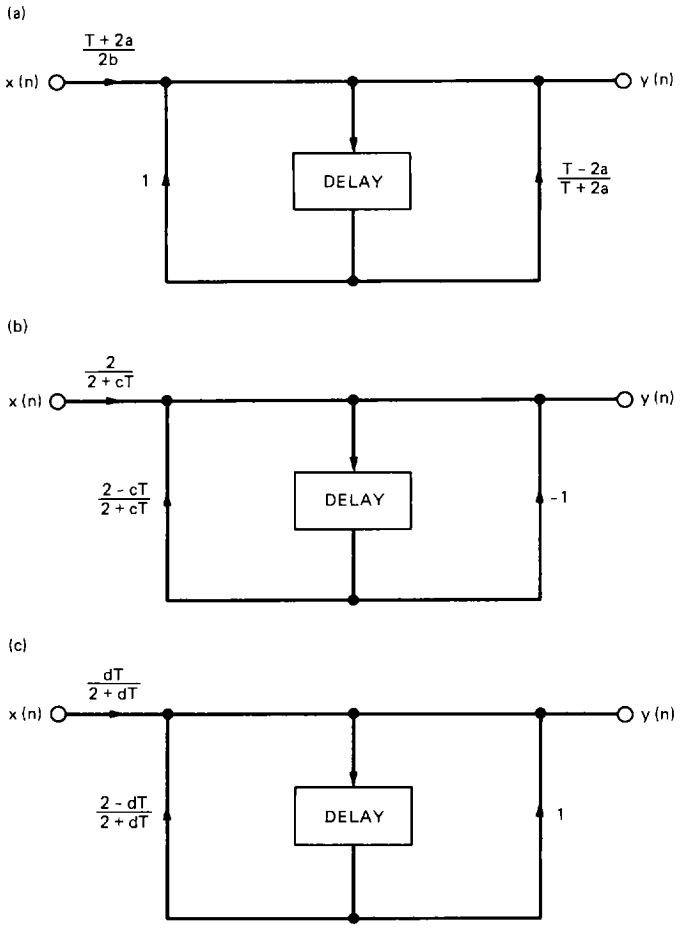

Fig. 2. Canonic form digital implementations: (a) loop filter; (b) high-pass filter; (c) low-pass filters

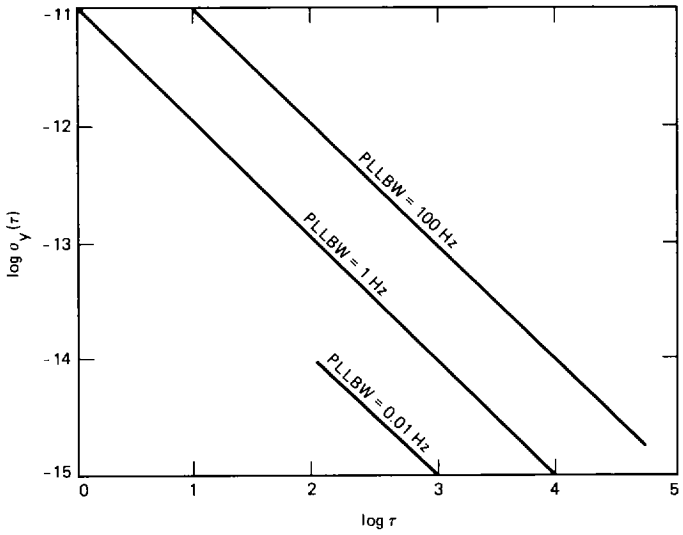

Fig. 3. General SNR-limited Allan variance